Iraq J. Electrical and Electronic Engineering
Vol. 1, No.1, 2001

المجلة العراقية للهندسة الكهربائية والالكترونية
مجلد ١، العدد ١، ٢٠٠١

Effect of System Impairment on the Performance of a Polarization Shift Keying Coherent Detection System Incorporating Jones Matrix Inversion Technique

R. S. Fyath and M. T. Rashid
Department of Electrical Engineering,
College of Engineering,
University of Basrah,
Basrah, Iraq.

Abstract

Recently, Jones matrix parameter shift keying (JMPSK) technique has been proposed in the literature to achieve phase noise and polarization state insensitive optical communication systems. The aim of this paper is to examine the performance of this system in the presence of system impairments, namely channel dichroism. A comprehensive analysis is presented to assess the effect of dichroism on the bit – error – rate (BER) characteristics of JMPSK receiver.

تأثير البارامترات الغير مثالية على أداء نظام الإزاحة المفتاحية للاستقطاب المتزامن والمستخدم لتقنية قلب مصفوفة جونز

الخلاصة

اثبت حديثا إن نظام (JMPSK) الذي يعتمد على الإزاحة المفتاحية للاستقطاب المتزامن (Coherent polarization shift keying) إضافة إلى تقنية قلب مصفوفة جونز (Inversion Jones matrix technique) له ثبوتية عالية ضد ضوضاء الليزر المستخدم في الإرسال والاستلام.

تقدم هذه الورقة دراسة لهذا النظام بوجود التأثيرات المختلفة وبالتحديد وجود الثنائية (Dichroism) المتولدة في القناة.

1 - Introduction

In coherent optical communication systems, the main problems affecting the receiver performance are laser phase noise and fluctuations of the state of polarization (SOP) of the optical field at the output of conventional single – mode fibers (SMFs) [1 – 4]. At presents, there is great interest in coherent systems that offer high immunity to both laser phase noise and SOP fluctuations with a limited penalty with respect to the quantum limit of conventional coherent systems. A mong these systems are [5]:

1. Antipodal Stokes parameter shift keying (ASPSK) system. This system is based on the property that orthogonal SOPs are antipodal criterion to demodulate

polarization modulated signal can be carried out by operating the decision in the Stokes space.

2. Jones matrix parameter shift keying (JMPSK) system. This system uses Jones matrix inversion technique at the receiver and it is based on the transmission of phase shift keying modulated signal and the reference optical carrier on two linear orthogonal SOPs. At the receiver, the transmitted polarizations are recovered by means of a pure electronic feedforward scheme so that no optical polarization control is needed.

The main contributions of this paper are:

- Comprehensive analysis is presented to assess the performance of JMPSK system in the presence of dichroism, birefringence, and coupling effects associated with the transmission optical channel.
- To compare the performance of both ASPSK and JMPSK system in the presence of system impairments.

The problem of dichroism arises in optical communication links due to the presence of polarization – dependent attenuation or/and optical amplification. Splices, couplers, switches, and semiconductor optical amplifiers usually show polarization–dependent characteristics [6]. The dichroism phenomenon seems to be present even in erbium - doped fiber amplifiers [6]. Thus we expect that dichroism becomes important when a large number of optical amplifiers is employed. Here, when a two orthogonally polarized waves are coupled to the fiber, the orthogonality is not assured between fiber output SOPs.

The simulation results presented here indicate clearly that JMPSK scheme is more robust against dichroism, birefringence and coupling effects compared with ASPSK system.

2 - Jones Matrix Parameter Shift Keying (JMPSK) System

The principle operation of this system depends on the inversion Jones matrix that estimated from the received signal. The effect of fiber propagation can be evaluated by means of Jones matrix J, a unitary operator which takes into account the polarization evaluation a long the fiber due to coupling between the polarization modes [7]. A block diagram of the JMPSK system is given in Fig. 1.

2.1 - System Description and Signal Analysis

A. The transmitter

At the transmitter, the laser field, which is assumed to be linearly polarized at angle $\pi/4$ with respect to reference axis, is divided into two components by the polarization beam splitter (PBS). The y-component is phase modulated between 0 and π by the message m(t), whereas the x-component is used as the reference carrier.

Let the optical laser field be expressed as:

$$E_{in}(t) = A_o e^{j(wt-\Phi_l(t))} \cos\theta \cdot \vec{x} + A_o e^{j(wt-\Phi_l(t))} \sin\theta \cdot \vec{y} \quad ....(1)$$

where A_o: Amplitude of the optical field.

Φ_l: Laser phase noise.

w : Transmitter optical angular frequency.

θ : Polarization angle with respect to reference axis.

These two field components at the input of the 2nd PBS are given by

$$E_x(t) = a_x e^{j(wt+\Phi_1(t))} \quad \text{.........(2a)}$$

$$E_y(t) = a_y e^{j(wt-\Phi_1(t)+\pi m(t))} \quad \text{.....(2b)}$$

where $a_x = A_o \cos(\theta)$ and $a_y = A_o \sin(\theta)$

$m(t)$: Modulated signal.

The output of the transmitter is given by

$$E(t) = [a_x \vec{x} + a_y e^{j(\pi m(t))} \vec{y}] e^{j(wt+\Phi_1(t))} \quad \text{....(3)}$$

B. The receiver

The optical field signal is carried by a SMF fiber characterized by a Jones matrix [J]. The received signal is expressed as

$$E_r(t) = [\vec{x} \quad \vec{y}][J] \begin{bmatrix} a_x \\ a_y e^{j\pi m(t)} \end{bmatrix} e^{j(wt+\Phi_1(t))} \quad \text{...(4)}$$

here the unitary matrix [J] is defined by [7]

$$[J] = \begin{bmatrix} \Gamma e^{jx_1} & \sqrt{1-\Gamma} e^{jx_2} \\ -\sqrt{1-\Gamma} e^{-jx_2} & \Gamma e^{-jx_1} \end{bmatrix} \quad \text{.....(5)}$$

In eqn. (5),

x_1, x_2: Phase shifts due to SMF effect and they are independent random variables with uniform distribution between 0 and π.

Γ^2: Variation of power due to SMF effect and it is a random variable with uniform distribution between 0 and 1.

The received optical field can be written as

$$E_r(t) = E_{rx}(t) + E_{ry}(t) \quad \text{........(6)}$$

where

$$E_{rx}(t) = [a_x \Gamma e^{jx_1} + a_y \sqrt{1-\Gamma^2} e^{j(\pi m(t)+x_2)}] e^{j(wt-\Phi_1(t))} \quad \text{...(7a)}$$

$$E_{ry}(t) = [a_y \Gamma e^{j(\pi m(t)-x_1)} - a_x \sqrt{1-\Gamma^2} e^{-jx_2}] e^{j(wt+\Phi_1(t))} \quad \text{...(7b)}$$

These two components E_{rx} and E_{ry} are mixed with the local laser field and then detected separately. The estimator circuit predicts the Jones matrix parameters. Then the matrix is inverted by an electronic adaptive circuit in order to separate the modulated signal from the reference carrier. Afterwards, the two signals are filtered by two IF filters F_1 and F_2 and the corresponding filter currents are given by

$$I_x(t) = 2a_x \Gamma e^{j(w_{IF}t+\Phi(t)+x_1)} + 2a_y \sqrt{1-\Gamma^2} e^{j(w_{IF}t+\Phi(t)+\pi m(t)+x_2)} + n_x(t) \quad \text{...(8a)}$$

$$I_y(t) = 2a_y \Gamma e^{j(w_{IF}t+\Phi(t)+\pi m(t)-x_1)} - 2a_x \sqrt{1-\Gamma^2} e^{j(w_{IF}t+\Phi(t)-x_2)} + n_y(t) \quad \text{...(8b)}$$

where

$w_{IF} = |w_t - w_{LO}|$: Intermediate angular frequency, with w_{LO} is the local oscillator angular frequency.

$\Phi(t)$: Difference between phase noise of the transmitter and local lasers.

$n_x(t)$, $n_y(t)$: Detection noise components.

The signals after the Jones matrix inversion and the IF filtering can be written as follows.

$$W_x(t) = 2a_x e^{j(w_{IF}t+\Phi(t))} + \Gamma[n_x(t) * h_1(t)] e^{-jx_1} - \sqrt{1-\Gamma^2}[n_y(t) * h_1(t)] e^{jx_2} \quad \text{....(9a)}$$

$$W_y(t) = 2a_y e^{j(w_{IF}t+\Phi(t)+\pi m(t))} + \sqrt{1-\Gamma^2}[n_x(t) * h_2(t)] e^{-jx_2} - \Gamma[n_y(t) * h_2(t)] e^{jx_1} \quad \text{....(9b)}$$

where $h_1(t)$ and $h_2(t)$ are the transfer functions of the IF filters F_1 and F_2, respectively, and * denotes convolution. The filter F_2 has a cutoff frequency equal to reference carrier, and a bandwidth $B = kB_L$, where k is proportionality constant and B_L is the sum of the linewidths for the transmitter and LO lasers. The filter F_1 acts on the modulated signal and it has a bandwidth $W = R + kB_L$, where R is the bit rate.

The decision variable q is obtained by beating $W_x(t)$ and $W_y(t)$ so that

$$q = 2\,\mathrm{Re}\{W_x^* W_y\} \quad \text{.................(10)}$$

2.2 - Evaluation of Bit - Error - Rate (BER)

The BER Pe can be calculated following a well-known analytical method [7] that has been applied for JMPSK system.

$$Pe = \frac{1}{2}\left[1 - Q(\sqrt{\xi_1}, \sqrt{\xi_2}) + Q(\sqrt{\xi_2}, \sqrt{\xi_1})\right] \quad \text{..(11)}$$

where Q(*,*) is the Marcum function and

$$\sqrt{\xi_1} = \frac{1}{2}\left(\sqrt{\frac{a_x^2}{2B}} + \sqrt{\frac{a_y^2}{2W}}\right)^2 \quad \text{....(12a)}$$

$$\sqrt{\xi_2} = \frac{1}{2}\left(\sqrt{\frac{a_x^2}{2B}} - \sqrt{\frac{a_y^2}{2W}}\right)^2 \quad \text{....(12b)}$$

$$Q(\sqrt{\xi_1}, \sqrt{\xi_2}) \approx \frac{1}{2}\,\mathrm{erfc}\left(\frac{\sqrt{\xi_2} - \sqrt{\xi_1}}{\sqrt{2}}\right) \quad \text{..(13a)}$$

$$Q(\sqrt{\xi_1}, \sqrt{\xi_2}) \approx 1 - \frac{1}{2}\,\mathrm{erfc}\left(\frac{\sqrt{\xi_2} - \sqrt{\xi_1}}{\sqrt{2}}\right) \quad \text{..(13b)}$$

Then the BER Pe can be expressed as

$$Pe \approx \frac{1}{2}\,\mathrm{erfc}\left(\frac{\sqrt{\xi_1} - \sqrt{\xi_2}}{\sqrt{2}}\right) \quad \text{......(14)}$$

where erfc(*) denotes the error function complement for the argument.

The received power is proportional to $a^2 = a_x^2 + a_y^2$ and $P = a^2/R$ is the number of detected photon per bit. If γ is the power splitting ratio for the PBS, then

$$P = \frac{a_x^2}{R\gamma} \quad \text{.......(15a)}$$

$$P = \frac{a_y^2}{R(1-\gamma)} \quad \text{.........(15b)}$$

The optimum value of γ that maximizing the argument of the BER is given by.

$$\gamma_{opt} = \frac{W}{B+W} = \frac{1 + k\frac{B_L}{R}}{1 + 2k\frac{B_L}{R}} \quad \text{........(16)}$$

Figure 2 shows the BER Pe versus the number of detected photons per bit where Pe is drawn using the optimum values of power splitting ratio. Note that Pe reduces with the increase of R/B_L. For $R/B_L = 10$ and P = 47 photons/bit, $Pe=10^{-9}$. For the ideal case where $R/B_L \to \infty$, P = 18 is needed to get $Pe=10^{-9}$.

In Fig. 3, we show the effect of power splitting ratio on the BER when P=47 photons/bit and $R/B_L=10$. The optimum value of γ (which makes $Pe=10^{-9}$) is 0.69. This result is an accord with that predicted by eqn. (16). The effect of R/B_L on the BER is drawn in Fig. 4, when P = 47 photons/bit. Note that Pe increases dramatically when R/B_L is reduced beyond 10. The optimum value of γ_{opt} as a function of R/B_L is plotted in Fig. 5. For low values of R/B_L, γ_{opt} tends to 0.5,where about one half of the transmitted power is carried by the reference carrier.

3 - Effect of Dichroism on JMPSK System

In this section, we show how the BER of JMPSK receiver is affected by dichroism. The results are based on a comprehensive signal analysis carried out for this system in the presence of dichroism.

3.1 Signal Analysis with Dichroism Effect: -

Assume that the optical signal is transmitted through a channel that presents random birefringence, coupling and dichroism. The received signals corresponding to m(t) = 0 (i.e. logic 0 is transmitted) and m(t) = 1 (i.e. logic 1 is transmitted) can be expressed as follows

$$E_{r0}(t)=\left[(a-\frac{\varepsilon}{2})\Gamma e^{j\chi_1}\cos\alpha+(a-\frac{\varepsilon}{2})\sqrt{1-\Gamma^2}e^{j\chi_2}\cos\alpha\right]e^{[j(wt+\Omega+\Phi_1(t))]}\bar{x}+\left[(a-\frac{\varepsilon}{2})\Gamma e^{-j\chi_2}\sin\alpha-(a-\frac{\varepsilon}{2})\sqrt{1-\Gamma^2}e^{-j\chi_2}\sin\alpha\right]e^{[j(wt-\Omega-\Phi_1(t))]}\bar{y} \quad ..(17a)$$

$$E_{r1}(t)=\left[(a+\frac{\varepsilon}{2})\Gamma e^{j\chi_1}\sin(\alpha+\frac{\varphi}{2})-(a+\frac{\varepsilon}{2})\sqrt{1-\Gamma^2}e^{j\chi_2}\sin(\alpha+\frac{\varphi}{2})\right]e^{\left[j(wt+\Omega+\frac{\rho}{2}+\Phi_1(t))\right]}\bar{x}-\left[(a+\frac{\varepsilon}{2})\Gamma e^{-j\chi_1}\cos(\alpha+\frac{\varphi}{2})+(a+\frac{\varepsilon}{2})\sqrt{1-\Gamma^2}e^{-j\chi_2}\cos(\alpha+\frac{\varphi}{2})\right]e^{\left[j(wt-\Omega-\frac{\rho}{2}-\Phi_1(t))\right]}\bar{y} \quad ..(17b)$$

where:

The IF signals at the electrical branches are

$$I_{xx0}(t)=2(a-\frac{\varepsilon}{2})\Gamma\cos\alpha\, e^{j(w_{IF}t+\chi_1+\Omega+\Phi_1(t))}+2(a-\frac{\varepsilon}{2})\sqrt{1-\Gamma^2}\cos\alpha\, e^{j(w_{IF}t+\chi_2+\Omega-\Phi_1(t))}+n_x(t) \quad ....(18a)$$

$$I_{yy0}(t)=2(a-\frac{\varepsilon}{2})\Gamma\sin\alpha\, e^{j(w_{IF}t-\chi_1-\Omega+\Phi_1(t))}-2(a-\frac{\varepsilon}{2})\sqrt{1-\Gamma^2}\sin\alpha\, e^{j(w_{IF}t-\chi_2-\Omega+\Phi_1(t))}+n_y(t) \quad ....(18b)$$

$$I_{xx1}(t)=2(a+\frac{\varepsilon}{2})\Gamma\sin(\alpha+\frac{\varphi}{2})e^{j(w_{IF}t+\chi_1+\Omega+\frac{\rho}{2}+\Phi_1(t))}-2(a+\frac{\varepsilon}{2})\sqrt{1-\Gamma^2}\sin(\alpha+\frac{\varphi}{2})e^{j(w_{IF}t+\chi_2+\Omega+\frac{\rho}{2}+\Phi_1(t))}+n_x(t) \quad ....(18c)$$

$$I_{yy1}(t)=-2(a+\frac{\varepsilon}{2})\Gamma\cos(\alpha+\frac{\varphi}{2})e^{j(w_{IF}t-\chi_1-\Omega-\frac{\rho}{2}+\Phi_1(t))}-2(a+\frac{\varepsilon}{2})\sqrt{1-\Gamma^2}\cos(\alpha+\frac{\varphi}{2})e^{j(w_{IF}t-\chi_2-\Omega-\frac{\rho}{2}+\Phi_1(t))}+n_y(t) \quad ....(18d)$$

The signal after the Jones matrix inversion and the IF filtering can be written as follows

$$W_{xx0}(t)=2(a-\frac{\varepsilon}{2})\cos\alpha\, e^{j(w_{IF}t+\Omega+\Phi_1(t))}+\Gamma[n_x(t)*h_1(t)]e^{-j\chi_1}-\sqrt{1-\Gamma^2}[n_y(t)*h_1(t)]e^{j\chi_2} \quad .....(19a)$$

$$W_{yy0}(t)=2(a-\frac{\varepsilon}{2})\sin\alpha\, e^{j(w_{IF}t-\Omega+\Phi_1(t))}+\sqrt{1-\Gamma^2}[n_x(t)*h_2(t)]e^{-j\chi_2}+\Gamma[n_y(t)*h_2(t)]e^{j\chi_1} \quad .....(19b)$$

$$W_{xx1}(t)=2(a+\frac{\varepsilon}{2})\sin(\alpha+\frac{\varphi}{2})e^{j(w_{IF}t+\Omega+\frac{\rho}{2}+\Phi_1(t))}+\Gamma[n_x(t)*h_1(t)]e^{-j\chi_1}-\sqrt{1-\Gamma^2}[n_y(t)*h_1(t)]e^{j\chi_2} \quad .....(19c)$$

$$W_{yy1}(t)=-2(a+\frac{\varepsilon}{2})\cos(\alpha+\frac{\varphi}{2})e^{j(w_{IF}t-\Omega-\frac{\rho}{2}+\Phi_1(t))}+\sqrt{1-\Gamma^2}[n_x(t)*h_2(t)]e^{-j\chi_2}+\Gamma[n_y(t)*h_2(t)]e^{j\chi_1} \quad .....(19d)$$

The decision variable q is obtained by the beating between W_{xx} and W_{yy} that described in eqn. (10).

3.2 - Evaluation of Bit - Error - Rate (BER)

One can evaluate the BER by using eqn. (11)

$$P_{em}=\frac{1}{2}\left[1-Q_m\left(\sqrt{\xi_{m1}},\sqrt{\xi_{m2}}\right)+Q_m\left(\sqrt{\xi_{m2}},\sqrt{\xi_{m1}}\right)\right] \quad ....(20)$$

where m(t) = 0, 1.

The total error probability is given by

$$P_{e}=\frac{P_{e0}+P_{e1}}{2} \quad ....(21)$$

$Q_m(\sqrt{\xi_{m1}}, \sqrt{\xi_{m2}})$ and $Q_m(\sqrt{\xi_{m2}}, \sqrt{\xi_{m1}})$ can be determined from the following equations.

$$Q_m(\sqrt{\xi_{m1}}, \sqrt{\xi_{m2}}) \approx \frac{1}{2}\,\mathrm{erfc}\left(\frac{\sqrt{\xi_{m2}}-\sqrt{\xi_{m1}}}{\sqrt{2}}\right) \quad \text{...(22a)}$$

$$Q_m(\sqrt{\xi_{m2}}, \sqrt{\xi_{m1}}) \approx 1-\frac{1}{2}\,\mathrm{erfc}\left(\frac{\sqrt{\xi_{m2}}-\sqrt{\xi_{m1}}}{\sqrt{2}}\right) \quad \text{...(22b)}$$

Then P_{em} can be expressed as

$$P_{em} \approx \frac{1}{2}\,\mathrm{erfc}\left(\frac{\sqrt{\xi_{m1}}-\sqrt{\xi_{m2}}}{\sqrt{2}}\right) \quad \text{.........(23)}$$

and

$$\sqrt{\xi_{m1}} = \frac{1}{2}\left(\sqrt{\frac{z_{xm}^2}{2B}}+\sqrt{\frac{z_{ym}^2}{2W}}\right)^2 \quad \text{..........(24a)}$$

$$\sqrt{\xi_{m2}} = \frac{1}{2}\left(\sqrt{\frac{z_{xm}^2}{2B}}-\sqrt{\frac{z_{ym}^2}{2W}}\right)^2 \quad \text{...........(24b)}$$

where

$$z_{xo} = a_x \cos\alpha \cos\Omega \quad \text{.....(25a)}$$

$$z_{yo} = a_y \sin\alpha \cos\Omega \quad \text{.....(25b)}$$

$$z_{x1} = a_x \sin(\alpha+\frac{\varphi}{2})\cos(\Omega+\frac{\rho}{2}) \quad \text{.....(25c)}$$

$$z_{y1} = a_y \cos(\alpha+\frac{\varphi}{2})\cos(\Omega+\frac{\rho}{2}) \quad \text{.....(25d)}$$

The power splitting ratio between a_x and a_y is computed from eqns. (15a) and (15b).

Figures 6 and 7 display the influence of dichroism parameters on BER P_e. The system parameter values used in the calculations are listed in Table 1. Note that the receiver performance degrades in the presence of dichroism. This result is illustrated further in Figs. 8 and 9 where the power penalty at $P_e = 10^{-9}$ is estimated as a function of ε and φ, respectively. Note that penalty exceeds 0.32 dB when φ approaches 60 ° and this effect is more pronounced in the presence of ε and ρ.

Table 1 Parameter values used to assess the performance of JMPSK system.

P_e	10^{-9}
p	47 photons / bit
R	10 G bit / s
B_L	1 GHz
α = Ω	0°
φ = ρ	0°
ε	0%

To show the effect of coupling parameter α and birefringence parameter Ω on BER characteristics, we plot the curves in Figs. 10 and 11, respectively. Investigating these plots reveals the following fact: The minimum BER is achieved when α = 0° and Ω = 0° or 180°.

4 - Discussions and Conclusions

In this section, the performance of JMPSK receiver is compared with that related to antipodal Stokes parameter shift keying (ASPSK) system. The ASPSK system has been proposed by Betti et al. [7] as a phase noise and polarization state insensitive coherent system and its performance has been addressed in the presence of dichroism by Betti et al. [6]. This system is based on the property that orthogonal polarization states are antipodal in the Stokes vector space. The system does not require optical polarization control and only electronic processing of the IF signals allows estimation of the position on the

Poincare sphere of the received SOP so that the decision can be made in an optimized way [7].

Table 2 compares the receiver sensitivity and dichroism - induced penalty for ASPSK and JMPSK systems. The parameter values used in the calculations are $P_e = 10^{-9}$, R = 10 Gbit/s and $B_L = 1$ GHz. The values of α and Ω are set to 45° (0 °) and 45° (0 °), respectively, for ASPSK (JMPSK) system. These values are optimum since the sensitivity attains the minimum level. Investigating Table 2 reveals the following findings.

(i). In the absence of dichroism, the JMPSK system gives 1.8 dB improvement in receiver sensitivity over ASPSK system.

(ii). The JMPSK system is more robust against dichroism effects than ASPSK system.

(iii). The sensitivity improvement gained by employing JMPSK system, over ASPSK system, increases in the presence of dichroism. When ε = 30%, φ = 60° and ρ=30°, the sensitivity improvement becomes approximately 2.4 dB.

Tables 3 and 4 summarize, respectively, the effect of α and Ω on the performance of ASPSK and JMPSK systems in the absence of dichroism. The parameter values of R, B_L and Pe used in the simulation are identical to those employed in producing the results in Table 2. The results in these tables indicate clearly that JMPSK system is more robust against variation of α and Ω compared with ASPSK system.

In conclusion, a comprehensive analysis has been given to assess the effect of dichroism on the bit – error – rate characteristics of JMPSK receiver. The results indicate clearly that this system is more robust against dichroism compared with ASPSK receiver.

5 - References

1. T. Okoshi and K. Kikuchi, "Coherent optical fiber communication", Tokyo: KTK Scientific Publishers, 1988, ch. 1.

2. W. H. C. De Krom, "Impact of laser phase noise on the performance of a {3 x 3} phase and polarization diversity optical homodyne DPSK receiver", J. Lightwave Tech., vol. 8, no. 11, Nov., pp. 1709-1715, 1990.

3. S. Benedetto and P. T. Poggiolini, "Multilevel polarization shift keying: Optimum receiver structure and performance evaluation", IEEE Trans. Commun., vol. 42., no. 2/3/4, Feb., pp. 1174-1186, 1994.

4. S. Bendetto and P. T. Poggiolini, "Theory of polarization shift keying modulation", IEEE Trans. Commun., vol. 40, no. 4, Apr., pp. 708-721, 1992.

5. S. Benedetto, R. Gaudino and P. Poggiolini, "Performance of coherent optical polarization shift keying modulation in the presence of phase noise", IEEE Trans. Commun., vol. 43, no. 2/3/4, Feb., pp. 1603-1612, 1995.

6. S. Betti, G. D. Marchis, E. Iannone, and F. Matera "Dichroism effect on polarization-modulated optical systems using Stokes parameters coherent detection", J. Lightwave Tech. Vol. 8, no. 11, Nov., pp. 1762-1768, 1990.

7. S. Betti, F. Curti, G. D. Marchis and E. Iannone, "Phase noise and polarization state insensitive optical coherent systems", IEEE J. Lightwave Tech., vol. 8, no. 5, May, pp. 756-767, 1990.

Table 2 Performance of ASPSK and JMPSK systems in the presence of dichroism effect.

Dichroism Parameters			ASPSK System		JMPSK System	
ε (%)	φ (deg.)	ρ (deg.)	Power (dBm)	Power penalty (dB)	Power (dBm)	Power penalty (dB)
0	0	0	-40.37	0	-42.2	0
0	0	30	-39.04	0.46	-42.14	0.08
0	30	60	-38.5	1	-41.87	0.34
30	30	0	-38.14	1.46	-41.5	0.8
30	60	30	-37.2	2.4	-41.1	1.2

Table 3 Performance of ASPSK system in the absence of dichroism for different values of α and Ω.

$P_e = 10^{-9}$, R = 10 Gbit/s, B_L = 1 GHz, ε = φ = ρ = 0.					
Ω = 45°			Ω = 30°		
α (deg.)	Power (dBm)	Power penalty (dB)	α (deg.)	Power (dBm)	Power penalty dB
45°	-40.37	0	45°	-40.37	0
40°	-39.1	1.27	40°	-38.7	1.66
35°	-38.24	2.13	35°	-37.11	3.26
30°	-37.1	3.27	30°	-34.88	5.5
α = 45°			α = 30°		
Ω (deg.)	Power (dBm)	Power penalty (dB)	Ω (deg.)	Power (dBm)	Power penalty (dB)
45°	-40.37	0	45°	-37.1	3.27
50°	-38.24	2.13	50°	-35.78	4.6
55°	-35.66	4.71	55°	-33.03	7.34
60°	-31.44	8.93	60°	-27.85	12.5

Table 4 Performance JMPSK system in the absence of dichroism for different values of α and Ω.

Pe = 10^{-9}, R = 10 Gbit/s, BL = 1 GHz, $\varepsilon = \varphi = \rho = 0$.					
$\Omega = 0°$			$\Omega = 15°$		
α (deg.)	Power (dBm)	Power penalty (dB)	α (deg.)	Power (dBm)	Power penalty (dB)
0°	-42.2	0	0°	-41.92	0.27
5°	-42.19	9.2*10 –3	5°	-41.88	0.31
10°	-42.1	0.11	10°	-41.78	0.41
15°	-41.92	0.27	15°	-41.62	0.57
$\alpha = 0°$			$\alpha = 15°$		
Ω (deg.)	Power (dBm)	Power penalty (dB)	Ω (deg.)	Power (dBm)	Power penalty (dB)
0°	-42.2	0	0°	-41.92	0.27
5°	-42.19	9.2*10 –3	5°	-41.88	0.31
10°	-42.1	0.11	10°	-41.78	0.41
15°	-41.92	0.27	15°	-41.62	0.57

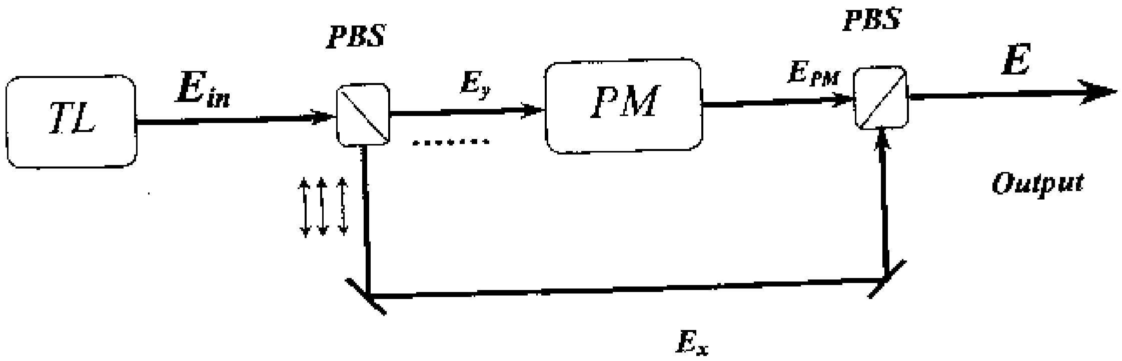

TL: Transmitter laser.

PBS: Polarization beam splitter.

PM: Phase modulator.

(a) Transmitter.

Fig. 1 Block diagram of the JMPSK system.

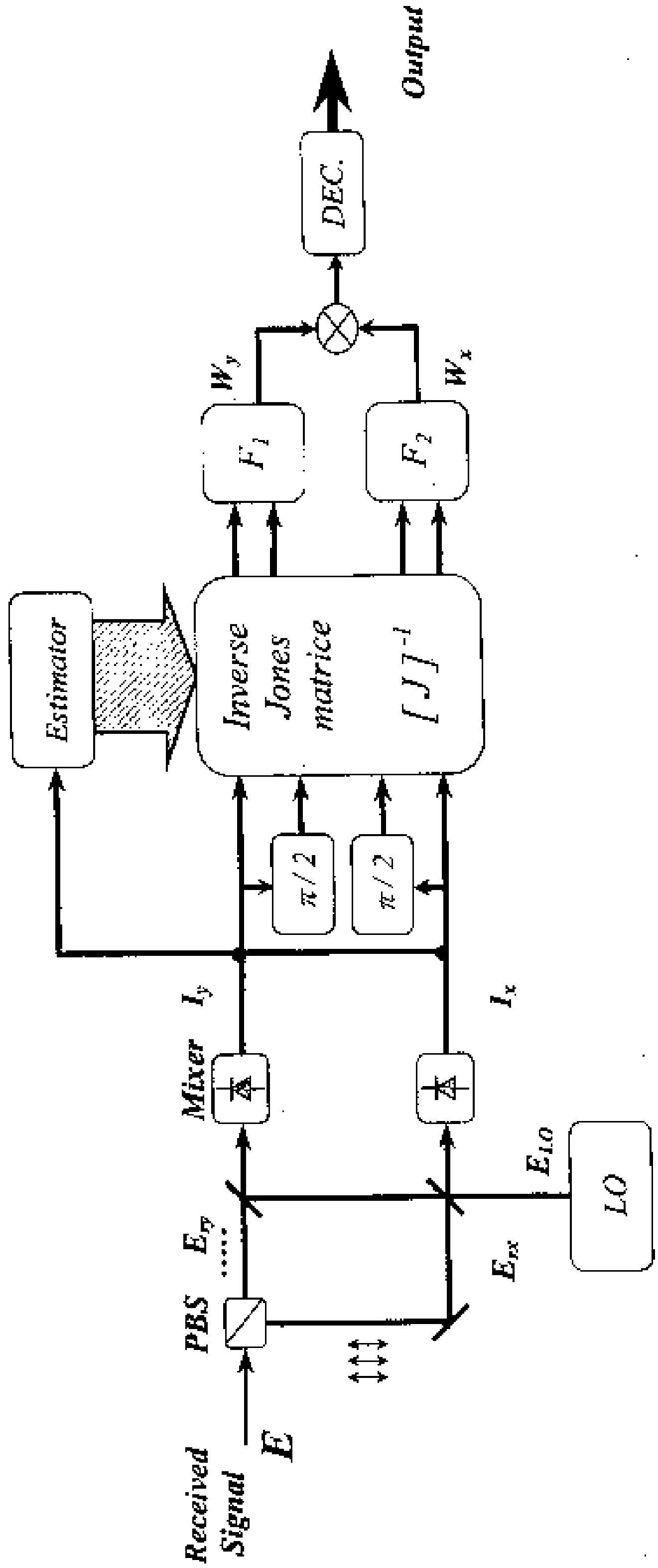

: Photodiode.

$[J]^{-1}$: Jones matrix inversion.

F_1, F_2: Two intermediate frequency filters.

LO: Optical local oscillator.

DEC.: Decision circuit.

(b) Receiver.

Fig. 1 (cont.)

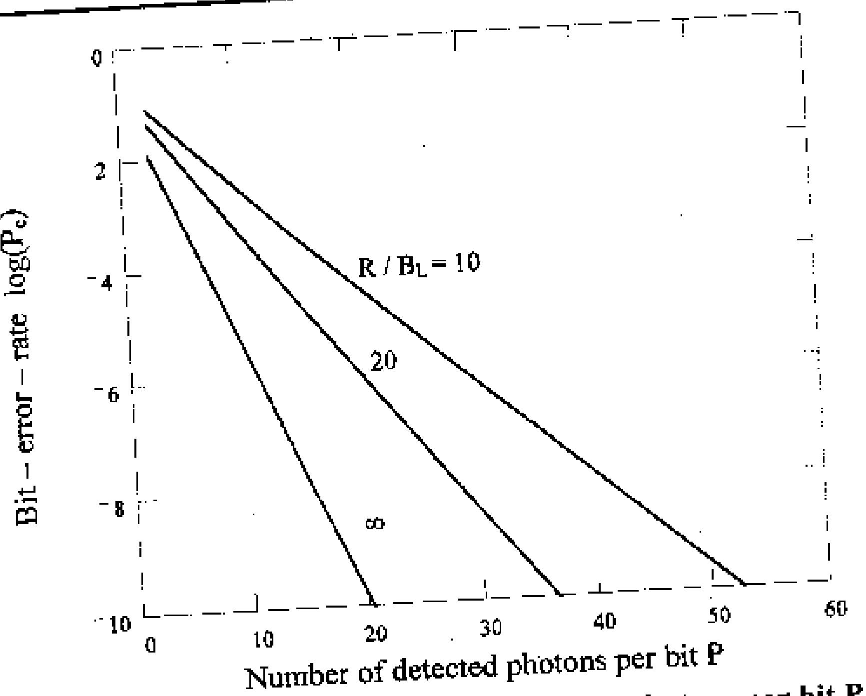

Fig.2 BER P_e versus the number of detected photons per bit P.

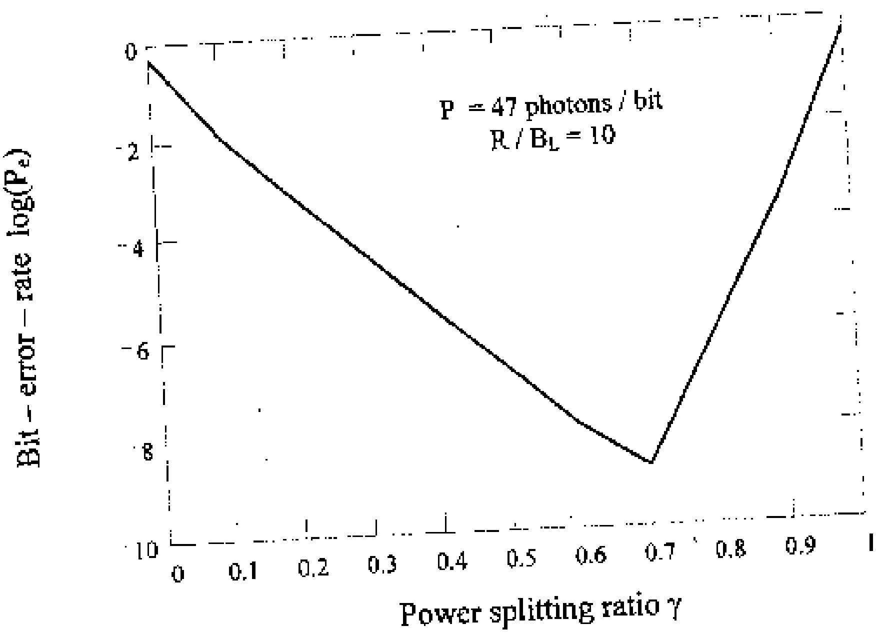

Fig. 3 BER P_e as a function of power splitting ratio γ.

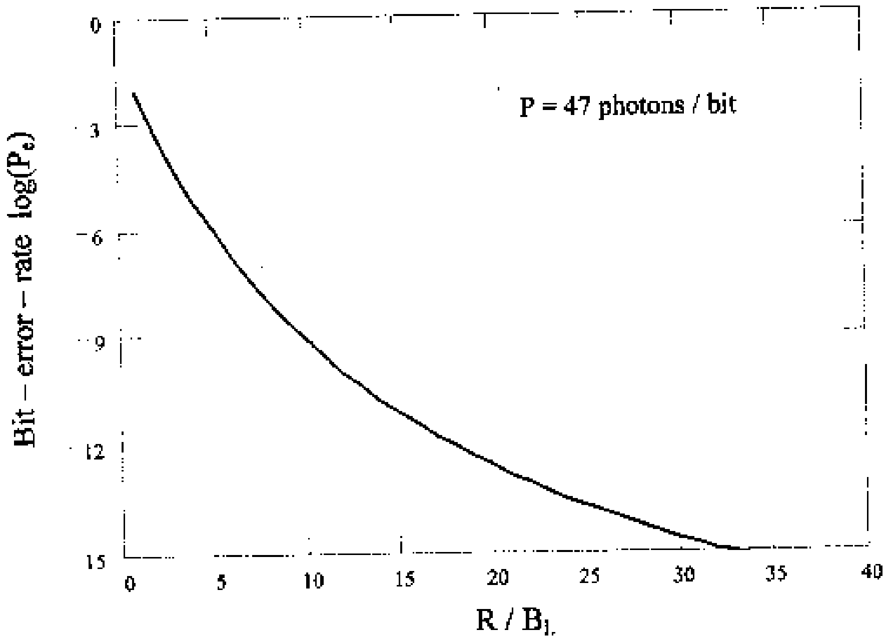

Fig. 4 BER P_e versus R / B_L .

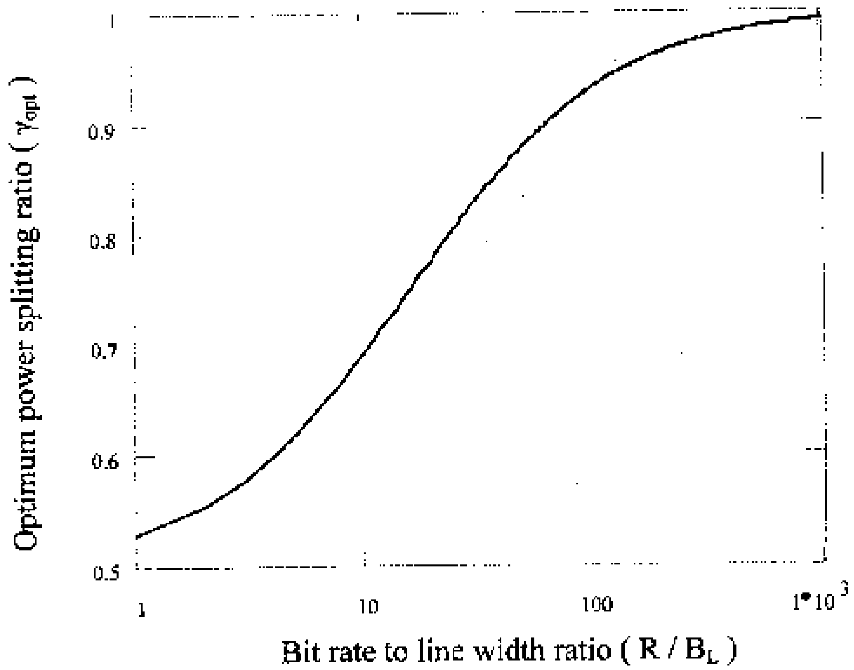

Fig. 5 Power splitting ratio γ_{opt} as a function of bit rate to linewidth ratio R/B_L .

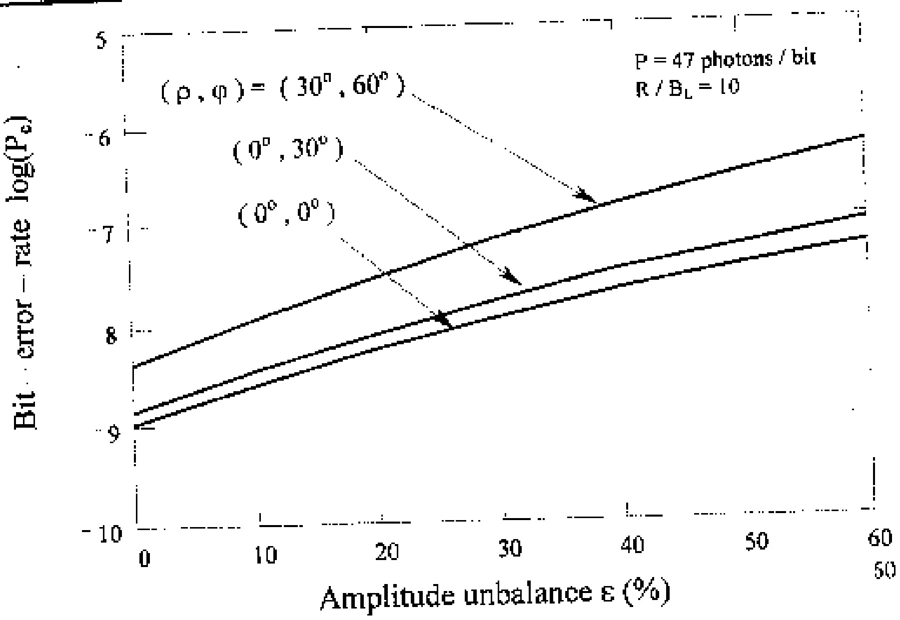

Fig. 6 BER P_e versus the dichroism-induced amplitude unbalance ε.

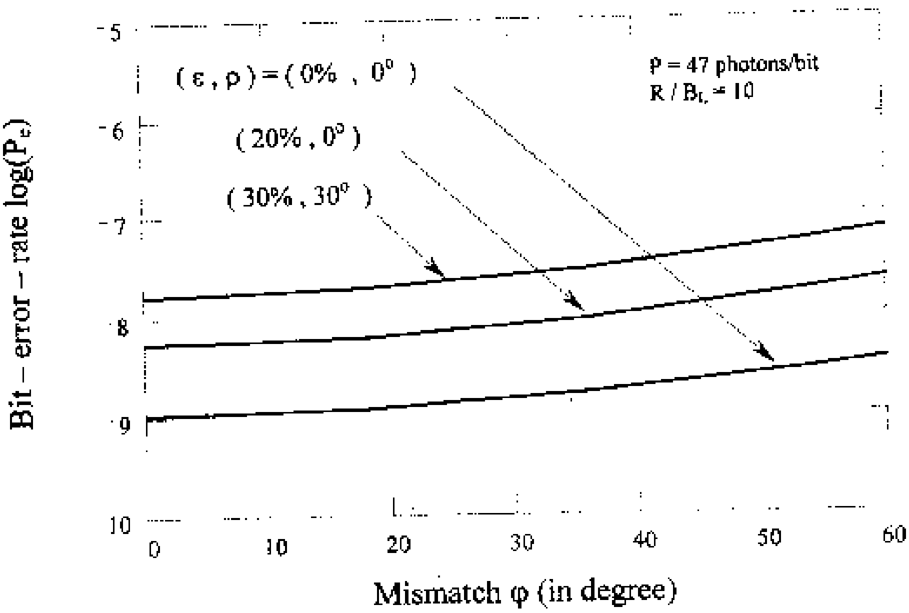

Fig. 7 BER P_e versus the dichroism – induced mismatch φ.

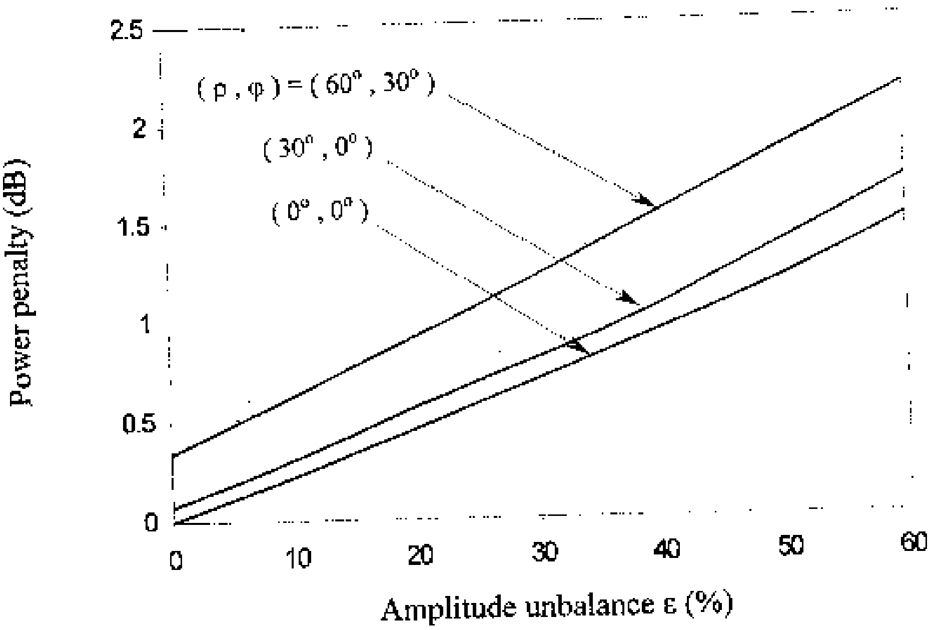

Fig. 8 Power penalty versus the dichroism – induced amplitude unbalance ε.

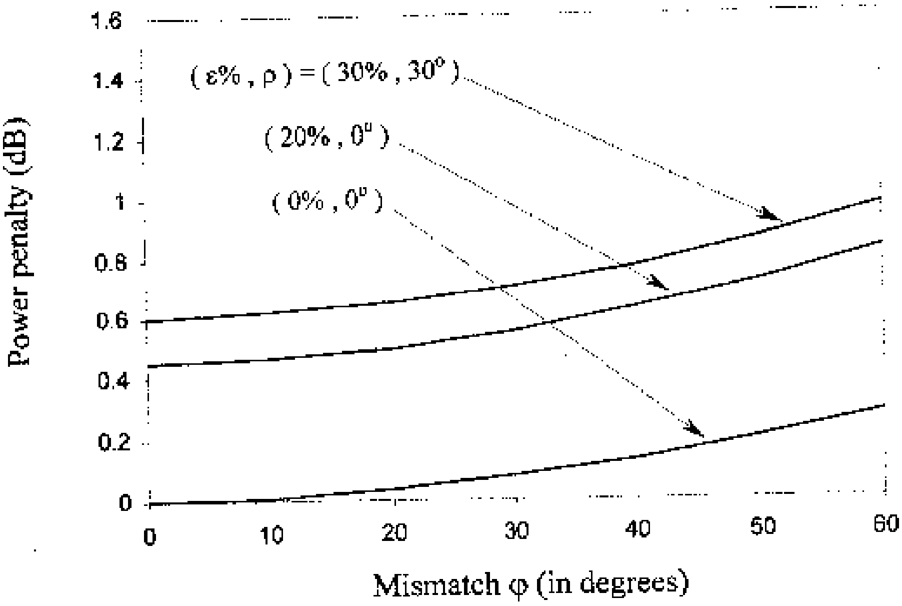

Fig. 9 Power penalty versus the dichroism – induced mismatch φ.

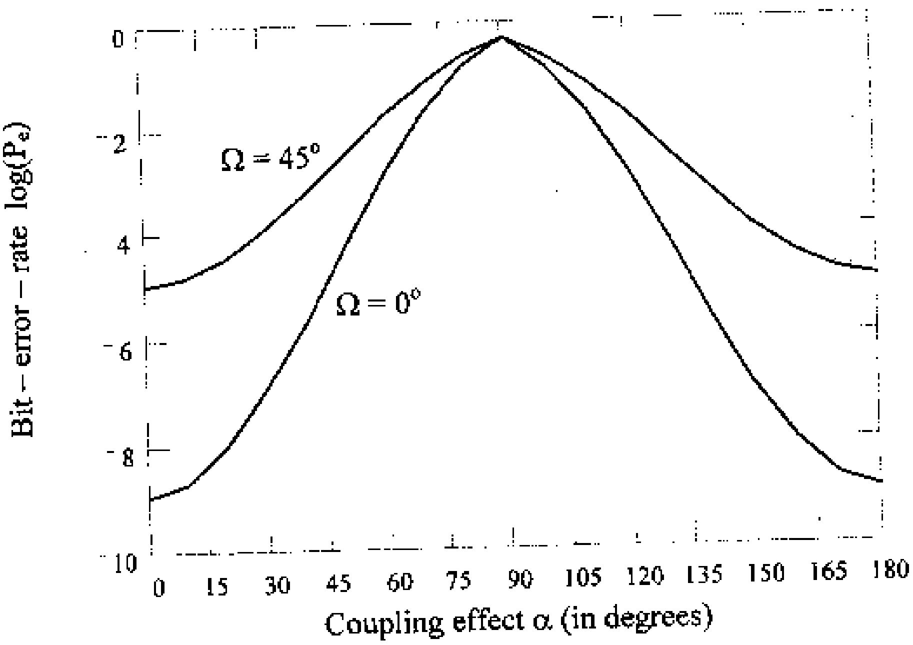

Fig. 10 BER P_e versus coupling effect α.

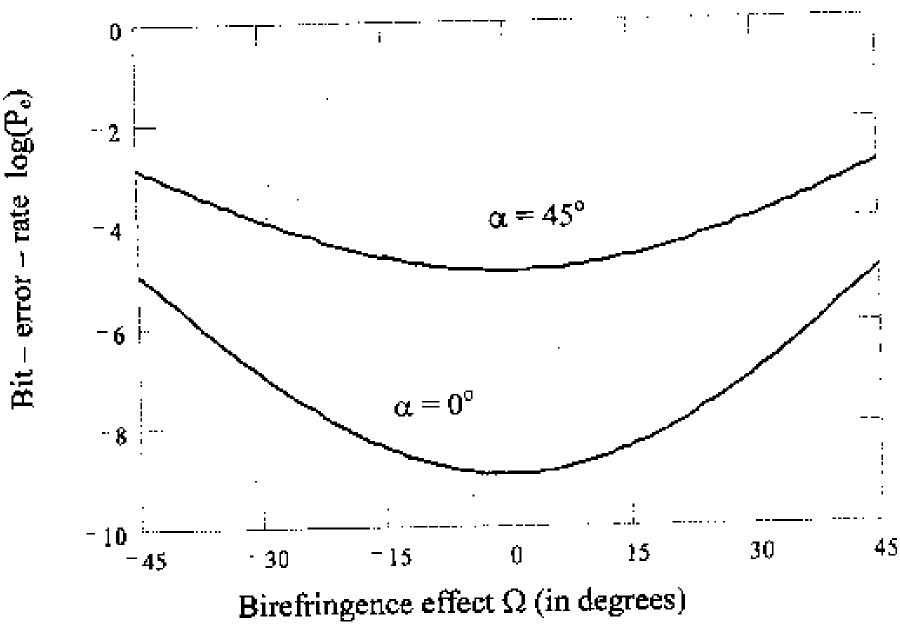

Fig. 11 BER P_e versus birefringence effect Ω.